Heliyon 5 (2019) e02561

Contents lists available at ScienceDirect

Heliyon

journal homepage: www.heliyon.com

Heliyon

Research article

Benquerencia (La Serena - Spain) rock art: An integrated spectroscopy analysis with FTIR and Raman

P. Rosina [a,*], H. Collado [b,c], S. Garcês [d], H. Gomes [d], N. Eftekhari [e], M. Nicoli [f], C. Vaccaro [e]

[a] Geosciences Center (UID_73) Polytechnic Institute of Tomar, Portugal
[b] ACINEP, Spain
[c] Geosciences Center (UID_73), Portugal
[d] Geosciences Center (UID_73), Portugal
[e] University of Ferrara, Department of Physics and Earth Science, Italy
[f] University of Ferrara, Department of Humanities, Italy

ARTICLE INFO

Keywords:
Archaeology
Materials chemistry
Analytical chemistry
Geosciences
Pigments
Recipes
Rock art
ATR-FTIR
Micro-Raman spectroscopy

ABSTRACT

La Serena region is a large plateau with open landscapes bounded in the south by a mountain chain formed by the Benquerencia, Tiros and La Rinconada Sierras. There are more than 300 painted and engraved sites in the region.

Cueva Grande, Cueva de En medio and Cueva Pequeña are three Schematic rock art shelters located in the municipality of Benquerencia de la Serena, Badajoz, Spain. Over their panels have been documented more than a hundred of painted schematic figures (anthropomorphic figures, eye-shape figures and symbols) (Neolithic – Copper Age).

Paintings are monochromatic with red or black coloration. A total of 13 samples (10 red and 3 black samples) from different panels were collected and analyzed using micro-Raman spectroscopy and ATR-FTIR.

Micro-Raman spectroscopy was able to characterize the main mineral component, respectively hematite for the red figures and charcoal for the black paintings. ATR-FTIR was useful to possible ochre and possible organic identification. These latest results are particularly important for understanding manufacturing processes and addressing conservation problems.

1. Introduction

In the last decade, analyses of prehistoric rock art have become widespread. The combination of different physic and chemical techniques and new methodological approaches has made it possible to determine raw material sources, operational sequences, pigments compositions, taphonomy processes, among other parameters, which can have direct implications on the rock art chronological framework.

The use of a multi-proxy is a common methodological approach to the pigment analyses (Franquelo et al., 2009).

Nevertheless, there are some studies linked to the characterization and identification of the organic binders and differential treatment of pigments (probably related to technical difficulties) (Iriarte et al., 2017), high degradation of the components and sites preservation (for binder identification cfr. López-Montalvo et al., 2017; Oliveira et al., 2017; Prinsloo et al., 2013).

The necessity to reduce the impact of the sampling on the panels made it only available a small collection of samples. This made it difficult to completely identify the pigments. Because of this, it was decided to apply micro-Raman spectroscopy and ATR-FTIR methods in order to characterize rock-art pigments from the Benquerencia de la Serena rock shelters, Badajoz, Spain.

1.1. Archaeological site and regional settings

Cueva Grande, Cueva de en Medio and Cueva Pequeña are located on the southern slope of the Sierra de la Buitrera (Fig. 1) a small Paleozoic quartzite mountain range with a hercynian orientation (NW-SE). Sierra de la Buitrera is part of an imposing mountainous barrier that separates the great plains of the Serena (along with Tiros, La Rinconada, La Osa and Las Vacas mountain range, which extend towards the East and the Benquerencia and Castuera mountain ranges which extend towards the west). All this area is articulated with the Zújar and the Guadiana valleys (which are located North of the mountainous barrier) and with the wide

* Corresponding author.
E-mail address: prosina@ipt.pt (P. Rosina).

https://doi.org/10.1016/j.heliyon.2019.e02561
Received 19 November 2018; Received in revised form 2 June 2019; Accepted 30 September 2019
2405-8440/© 2019 Published by Elsevier Ltd. This is an open access article under the CC BY-NC-ND license (http://creativecommons.org/licenses/by-nc-nd/4.0/).

Fig. 1. Location of Sierra de la Buitrera, Badajoz, Spain.

natural corridor of the Pedroches, located South of the mountains. This is considered to be one of the most important communication routes between the average basin of the Guadalquivir River and the upper course of the Guadiana River.

Possibly the choice of these shelters, besides its remarkable conditions as a refuge, was conditioned by its excellent strategic position, framed between two important points of passage (Puerto Mejoral on West and Puerto de la Nava on East).

This position allows the transits in N–S direction through the mountainous areas for the traditional itineraries of transhumant huts. From the rock shelters presented here, there is an excellent visual control on all these roads.

The nearby archaeological context indicates an intense occupation of the territory during the recent prehistoric times, with large high-altitude settlements such as Cerro del Montón, Castillejo de la Nava, Las Moriscas or Cerro Mejoral and others of lesser importance such as the Cueva de los Pinos, Valdejazmin or Cueva de los Vencejos whose surface materials reveal a wide chronological range between the end of the Neolithic and the Late Bronze-Early Iron Age, although with a special intensity throughout the Copper and Bronze Ages (Pavón Soldevila et al., 2018).

The graphic set is remarkable (Fig. 2); 9 decorated panels have been documented both in Cueva Grande and Cueva de En Medio shelters. 4 decorated panels have been documented in Cueva Pequeña. All the figures are painted, mainly using pigments of red tones and even if in a much smaller proportion, black pigments. These latter are located almost entirely in the Cueva Pequeña. Direct finger painting is the main technique applied to all the rock shelters which generated a stroke of around one centimeter in thickness on the majority of the paintings. However, there are figures executed with a much finer stroke, (not exceeding 3–4 mm), which indicates that some fine-tipped instruments were used to apply the paint on the wall as well. Especially in Cueva Grande shelter is remarkable the size of the paintings (some motifs are 40cm high), which are larger than the average size known for Schematic rock art figures (between 10 and 20 cm high).

The iconography is varied and clearly fits into the Iberian Peninsula artistic horizon so-called "Schematic Rock Art". It should be noted that zoomorphic figures are absent in all shelters. Apart from that, human representations of different types appear in all shelters along with a wide range of symbolic figures with a big presence of aligned groups of vertical bars and clouds of finger prints, both in red and black colors. It is important to highlight the existence in Cueva de En Medio of a magnificent representation of the Eye-Shape Idol figure whose comparisons with mobile archaeological objects clearly indicate us a Final Neolithic horizon - Full Copper Age chronology.

Finally, taking into account only iconographic criteria, there seems to be in this set of rock shelters a kind of "identity sign", created by the repeated representation of motifs with a similar basic scheme.

2. Materials and methods

2.1. Sample collection

Thirteen pigment samples were collected from the 3 rock art shelters to be analyzed with micro-Raman spectroscopy and ATR-FTIR. Samples included ten red pigments (Cueva Grande and Cueva de En Medio), and three black pigments (Cueva Chica). ATR-FTIR analyses were carried out only in the ten red pigments because after micro-Raman spectroscopy results, it was decided to keep the samples of charcoal for absolute dating (Fig. 3).

These samples were collected in strategic figurative motifs, in order to encompass all the typological spectrum of the motives and taking into account the variation of the colour (white, black and various shades of red). Where possible, sample collection has been done using non-contact ethical extraction techniques (applying the code of ethics and guidelines for practice of American Institute for conservation). Each sample, weighing between 10 and 100 mg, was extracted in areas of the panel where pigment was easily observed or in areas with fractures. Each sample was obtained using a sterilized tungsten scalpel and inserted in a 0,5ml microcentrifuge tubes.

2.2. Instrumental

Micro-Raman spectroscopy was employed to determine the mineralogical composition of pigment samples. Micro-Raman measurements were performed by LabRam HR800 spectrometer (Horiba Jobin Yvon, France), coupled with an Olympus BXFM optical microscope (Olympus, Tokyo, Japan). The spectrometer was equipped with an air-cooled CCD detector (1024 × 256 pixels) at –70 °C, it had a focal length of 80 mm and was equipped with two 600 and 1800 grooves/mm gratings. The laser beam diameter of the instrument was about 1 mm and the resolution of the spectrometer was approximately 4 cm^{-1}.

The He–Ne laser line at 632.82 nm was used as excitation source and was filtered to keep the laser power varying from 0.2 to maximum 10 mW. Exposure time, beam power and accumulations were optimized for each sample in order to obtain sufficiently informative spectra but ensuring to avoid alteration of the sample. Several measurements were performed at low laser powers and increasing it gradually, where possible. A severe problem, in fact, is that some iron minerals are transformed easily when applying laser powers greater than 1 mW. Most of the iron (oxy)hydroxides can be converted to haematite, without realizing that a transformation took place. This fact can impede a reliable identification of the original material, when using a not appropriate laser

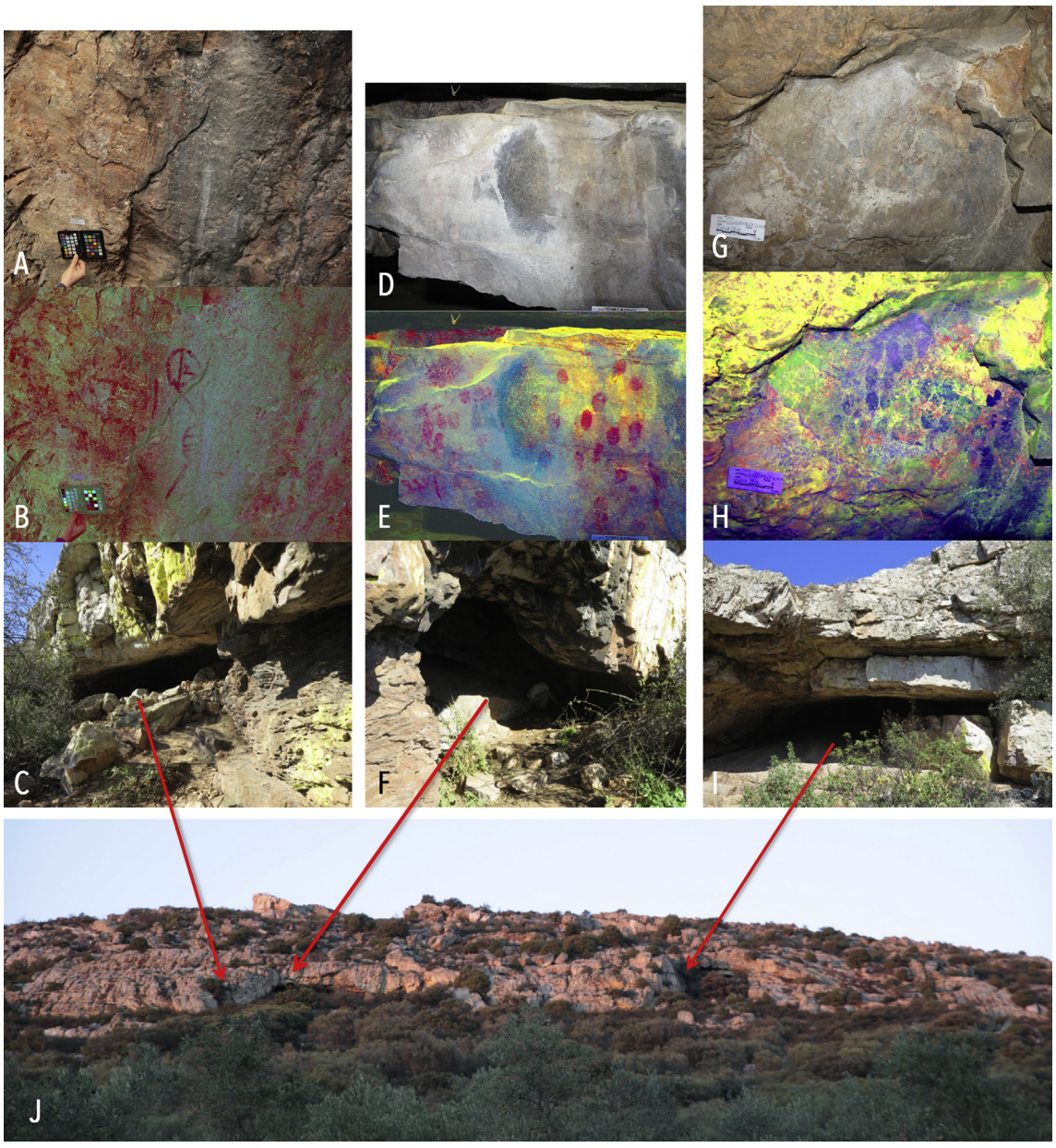

Fig. 2. Shelters and paintings from A) Cueva Grande; B) Cueva de en El Medio and C) Cueva Pequeña.

power (Hanesch, 2009).

Raman spectra were recorded in the range of 200–2000 cm^{-1} with an exposure time of 5–16 s and 5–11 accumulations. The 10x and 50 x microscope objectives were employed to focus the laser beam onto the samples, placed on the X–Y motorized sample holder, and the spot size diameter was about 2–3μm. The wavelength scale was calibrated using a Silicon standard (520.5 cm^{-1}) and the acquired spectra were compared with scientific published data and reference databases, such as Horiba LabSpec 5 (Horiba) and RRUFF (RRUFF, University of Arizona, AZ, USA).

ATR-FTIR spectra of samples were collected using a Bruker Alpha FT-IR, Opus 7.5 software, spectrometer employing an ATR (Attenuated Total Reflection) sampling device. The ATR-FTIR spectrometer was equipped with a global source, a KBr beam splitter, and a Deuterated Lanthanum α Alanine doped TriGlycine Sulphate detector in room temperature. The ATR sampling device worked with a diamond internal reflection element (IRE) in a single-reflection configuration. Spectra were recorded over the spectral range of 400–4000 cm^{-1} at a 4 cm^{-1} resolution, 24 scans.

3. Results and discussion

3.1. Cueva Grande

3.1.1. BSQG-1

ATR-FTIR analysis for sample BSQG-1 revealed only typical spectra of quartz (RRuff database), probably belonging to quartzite substrate; while micro-Raman spectrum revealed hematite, with the typical Raman bands at about 225, 240, 295, 406, 492, 605, 657, 1320 cm^{-1} (Hernanz et al., 2012; Iriarte et al., 2013) (Fig. 4a). It should be pointed out that in literature the peak at 656 cm^{-1} has been subject to different interpretations. Some studies attribute this peak to a disordered phase of hematite (Iriarte et al., 2017; Hunt et al., 2018). However, in many cases, the same peak can be attributed to the mineral phase of magnetite (Fe_3O_4), as reported by Froment et al. (2008) and Rousaki et al. (2015).

In the micro-Raman spectrum, the peak at 467 cm^{-1}, attributable to the presence of quartz, it is a confirmation of the ATR-FTIR results (Fig. 6a-1).

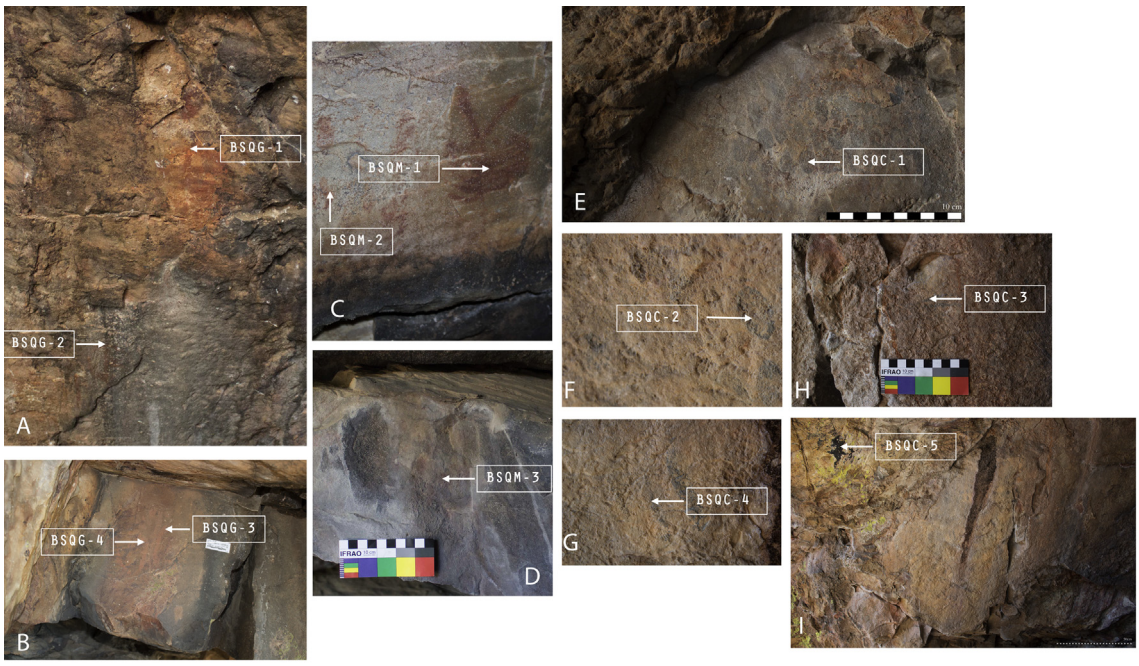

Fig. 3. Panel with black fingerprints from Cueva Pequeña.

3.1.2. BSQG-2

On sample BSQG-2 the presence of hematite was confirmed by both ATR-FTIR and μ-Raman. The ATR-FTIR spectrum, in fact, beside the presence of quartz, shows a band at 548 m cm^{-1}, attributed to hematite (Legodi and Waal, 2006) (Fig. 4b). Raman bands at 223, 243, 291, 405, 489, 602, 656, 1320 cm^{-1} confirm this result, suggesting also the possible presence of magnetite in the sample, due to the peak recorded in the spectrum at 656 cm^{-1} (Fig. 6a-2).

3.1.3. BSQG-3 and 4

The composition of the red figure of sample BSQG-3 shown by ATR-FTIR (Fig. 4c) is certainly more interesting and more complex: pigment is formed by clay and an organic substance. Distinct ATR-FTIR bands of clay are 1032vs (Si–O stretching in clay minerals) and 3694w cm^{-1} (O–H bond) (Ekosse, 2005). C–N stretching (band 1508 cm^{-1}), C=O bond of ester (band 1727 cm^{-1}), the CH stretching (bands 2788 cm^{-1} and 2926cm^{-1}) point out for organic matter, probably of vegetal origin (Ch'ng et al., 2016). In rock art painting organic matter could also derive from lichens or biomineralization (Buzgar et al., 2009) but presence of band at 3362sh cm^{-1}, signaled in clay modified by organic intercalation (Frost et al., 2002; Hu et al., 2015), suggests that this substance is part of pigment as binder or even dye.

For what concern μ-Raman analyses (Fig. 6a-3) on this sample, the main result is the presence of hematite. The recorded spectrum shows, as for the previous cases, the 608-657 cm^{-1} doublet, which suggests the presence of magnetite. The aspect of the spectrum together with the presence of clay, recorded by ATR-FTIR, allow assuming the use of red ochre as a raw material for the preparation of the pigment, supporting the results previously obtained by Prieto and Jiménez (2000).

Red ochre is a rock or natural earth with a variable mineralogical composition, which color results from the presence of iron oxides. Although the iron oxides and hydroxides are the main constituent of this raw material, the purity of ochre can vary and other minerals such as quartz, clays, gypsum, micas, feldspars, etc. can be detected in the matrix (Bikiaris et al., 2000; Eastaugh et al., 2008). The characterization of red ochre from the prehistoric paintings of Tito Bustillo Cave and the Monte Castillo Caves (Northern Spain), carried out by Iriarte et al. (2009), shows that, even if a ochre has a very low Fe content, in respect to the content of clay, it can result in a red color. In fact, Fe concentrations as low as 0.1% are sufficient to give ochres a red color (Cornell and Schwertmann, 2006).

Magnetite can be also found in red ochre, inducing slight changes in the intensity of color shades, as observed by Froment et al. (2008) and Zuo et al., (1999). In particular, for what concerns the red ochre from Spanish rock art, has been noticed by Hernanz et al. (2008) presence of magnetite.

The last sample of this rock shelter (BSQG-4) was collected from the patina that covered the underlying painting. ATR-FTIR analysis (Fig. 4d) had shown presence of phosphates (bands 504, 535, and 567 cm^{-1}) (Schiegl and Conard, 2006). On the other hand, micro-Raman analyses revealed the characteristic peaks of hematite at 224, 243, 289, 406, 491, 605, 656, 1320 cm^{-1}, probably due to the presence of small traces of pigment trapped in the patina (Fig. 6a-4).

3.2. Cueva en el medio

3.2.1. BSQM-1

ATR-FTIR analysis on sample BSQM-1 (Fig. 5a), collected from the eye-shape idol figure, revealed only quartz, pertaining to the substrate, with the same bands of BSQG-1. The sample comes from a red figure and is of a red color when observed under the optical microscope. The Raman analysis, in fact, revealed on this sample the presence of hematite with the typical Raman peaks at 219, 238, 289,404, 608, 655 cm^{-1} (Hernanz et al., 2012; Iriarte et al., 2013) (Fig. 6b-1).

3.2.2. BSQM-2

ATR-FTIR organic bands (2851, and 2921 cm^{-1}) of the reddish fingerprints BSQM-2 (Fig. 5b), should correspond to any herbs (Ch'ng et al., 2016; Omotoso and Ajagum, 2016). Spectrum displayed presence of quartz and possibly clay (characteristic band at 1060vs cm^{-1}). Peak at 1315 should be attributed at calcium oxalate. Absence of OH bands over 3000 cm^{-1} could be an indication of heating (Schuttlefield et al., 2007). The fluorescence observed at micro-Raman and the impossibility of detecting spectra for this sample is compatible with the presence of organic matter and oxalates, detected by ATR-FTIR.

3.2.3. BSQM-3

ATR-FTIR on sample BSQM-3 (Fig. 5c) showed a C–H stretching

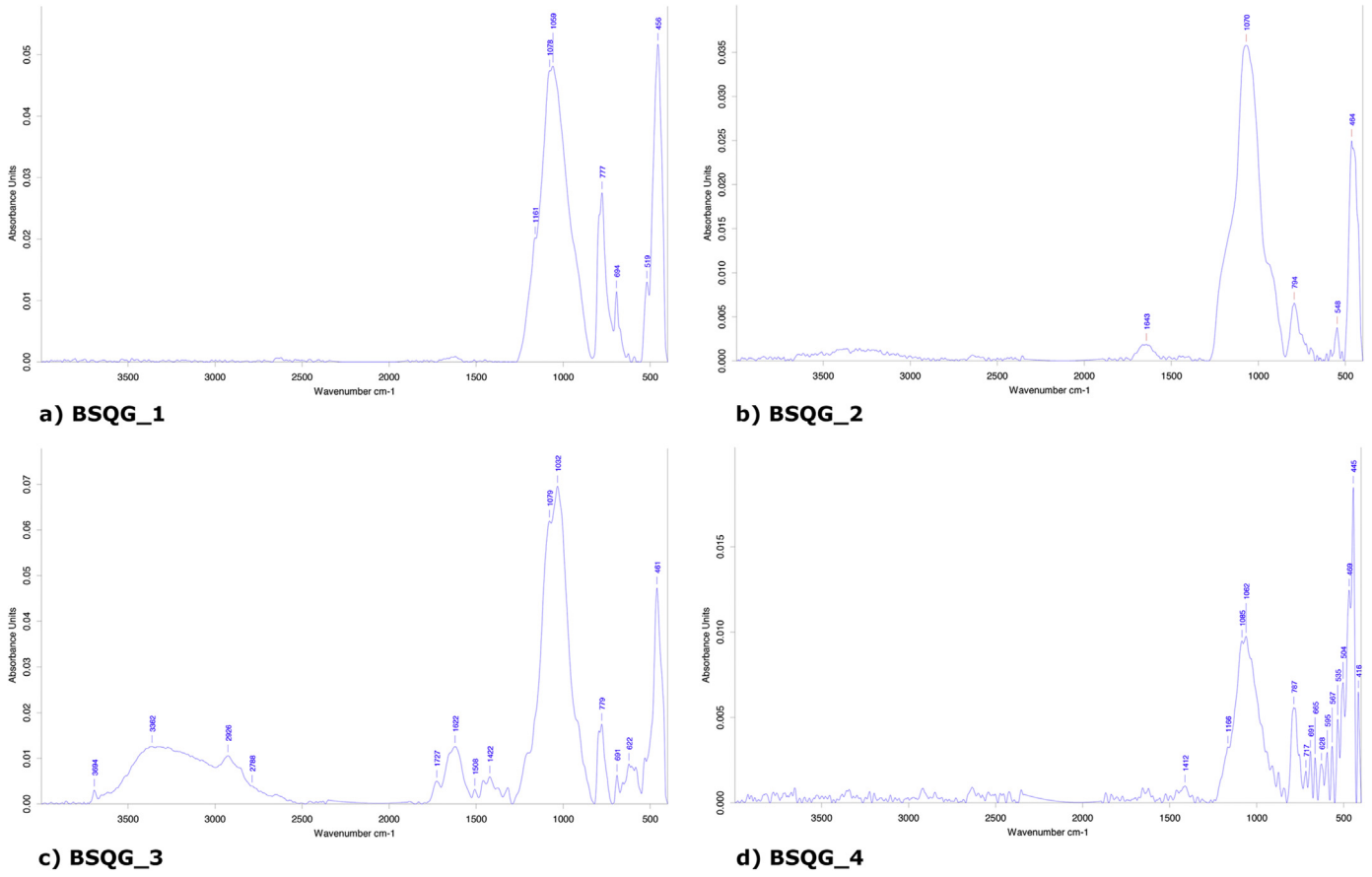

Fig. 4. ATR-FTIR spectra of Cueva Grande.

(band 3159 cm^{-1}), probably corresponding to an impurity of the substrate. However, the presence of pigment, has been detected by μ-Raman (Fig. 6b-3) that shows in the spectrum the typical bands of hematite at 221, 291,407,494, 608, 665 cm^{-1}. This is plausible as the sample, also in this case, comes from a red fingerprint figure.

3.2.4. BSQM-4

Spectra of BSQM-4 (Fig. 5d) represent most likely another recipe. In fact, clay (bands 441vs e 1045sh cm^{-1}), is mixed with hematite (band 558 cm^{-1}), as recorded by Raman spectroscopy (Figs. 6b-4) and an organic substance (bands 2350, 2454, and 2651 cm^{-1}), recorded by micro-ATR-FTIR. Organic ingredient could be attributed to pyridine (Rospenk and Zeegers-Huyskens, 1997); this component is present in some herbs roots and some marshmallows but is also present in different organic compounds.

The Raman spectrum recorded from this sample shows the typical peaks of hematite at 218, 240, 289, 403, 488, 604 cm^{-1}, confirming the result obtained by ATR-FTIR. Moreover, the spectrum shows the peak at 656 cm^{-1} attributable to the presence of magnetite. As considered for the sample BSQG-3 of Cueva Grande, these features, together with the presence of clay recorded by ATR-FTIR, suggest a possible use of red ochre as a raw material for the manufacturing of the pigment.

ATR-FTIR band 1040 cm^{-1}, therefore, should be attributed to red and white clay of mixed origin (Sathya et al., 2012). It is not possible to neglect the temperature influence of bands distortion (Cakraborty and Ghosh, 1991).

3.2.5. BSQM-5

The case of sample BSQM-5 is very similar to what observed for samples BSQM-1 and BSQM-3. ATR-FTIR analysis (Fig. 5e), in fact, showed only phases pertaining to the substrate, while μ-Raman spectrum (Fig. 6b-5) of the sample showed the typical peaks of hematite at 221, 243, 291, 408, 494, 608, 659 cm^{-1} and a small peak at 462 cm^{-1} corresponding to quartz, the main constituent of the rocky panel.

3.2.6. BSQM-6

The large figure analyzed with ATR-FTIR in sample BSQM-6 was painted with dehydrated clay (Che et al., 2011), possibly red ochre, and a nitrogen substance. Presence of phosphorus and nitrogen could be related with the very same composition of the red soil (Niederb et al., 2015) (Fig. 5f).

Raman analysis for this sample shows the mineral phase of hematite (218, 240, 288, 404, 608, 661 cm^{-1}). This result, as for sample BSQG-3 and BSQM-4, can be correlated with the presence of clay detected by ATR-FTIR and suggests the use of red ochre as a pigment.

3.3. Cueva Chica

The three samples collected from Cueva Chica come from three different black figures painted several panels. Sample 1 was taken from a group of finger marks, sample 2 comes from another group of finger marks near the entrance, and sample 3 was collected from two horizontal black lines more internally.

On these samples, only μ-Raman analysis was carried out (Fig. 6c) in order to preserve the samples for possible future dating. All the three samples, in fact, showed the broad Raman band at about 1353 and 1595 cm^{-1} that are attributable to amorphous carbon.

It should be noted that Raman bands of amorphous carbon can vary due to the intrinsic features of a material and due to the differences in the measuring process (Coccato et al., 2014). However, in all the spectra

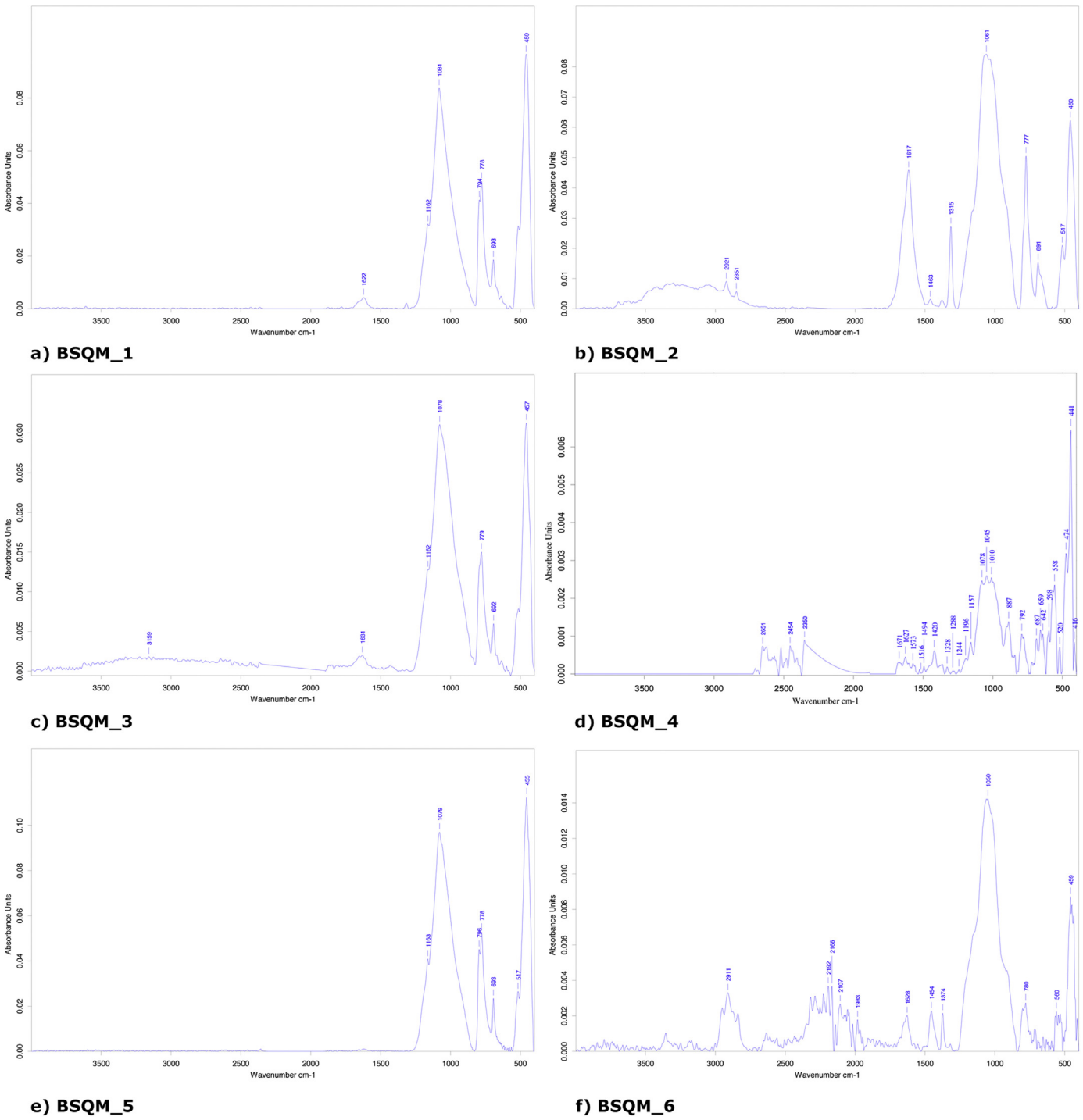

Fig. 5. ATR-FTIR spectra of Cueva en el Medio.

recorded for the three samples of black pigment were detected the broad bands of disordered carbon in the spectral region 1000-1600 cm^{-1}, according with literature (Iriarte et al., 2013; Wainright et al., 2002; Hernanz et al., 2008; Gomes at al., 2013). These results suggest the use of charcoal or soot probably derived from the combustion of vegetable materials.

4. Conclusions

The color palette of the Iberian prehistoric paintings in the post-paleolithic period is essentially composed by red pigments in their various shades, black, yellow and white. Essentially they are all monochromatic.

Several important considerations could be made from these results. First, there is a clear evidence of the limitation of the sample itself in some cases. Hematite was used as the basis for red coloration without any doubt, just as charcoal was used as the basis for black coloration. However, in several samples, ATR-FTIR presents no results (BSQM-1,3,5). Having said that, it is clear that using only the micro-Raman, all the samples appear as hematite, but comparing the ATR-FTIR results it is

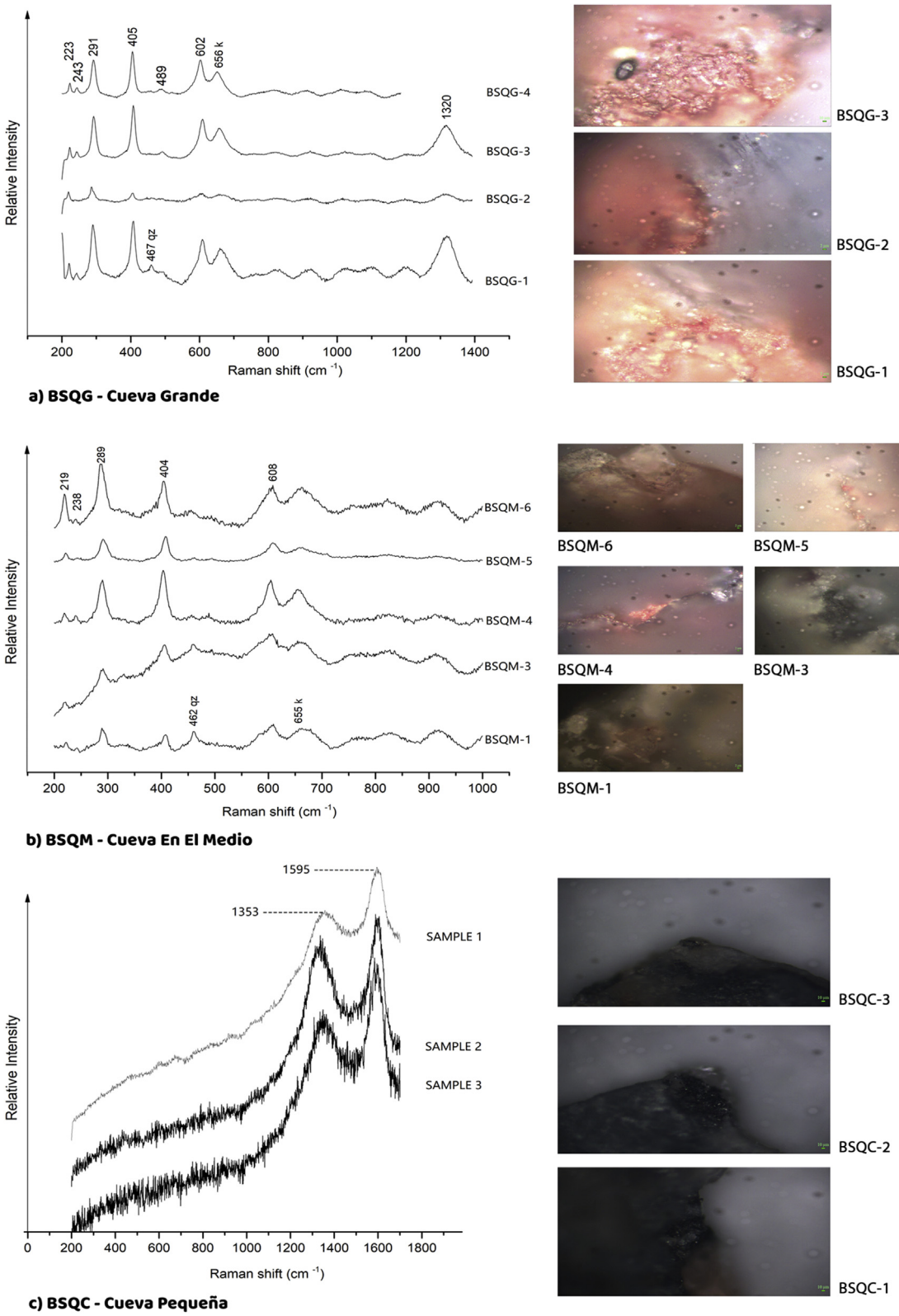

Fig. 6. Micro-RAMAN spectra of Benquerencia de la Serena shelters: a) BSQG - Cueva Grande; b) BSQM - Cueva En El Medio; c) BSQC - Cueva Pequeña.

observed that the paintings may have been made using clays and possibly by joining organic materials. The complementarity of micro-Raman and micro-ATR-FTIR techniques allowed in at least three cases (BSQG-3, BSQM-4, BSQM-6) to correlate different data and so to assume the use of red ochre as a source material for the pigment production. This is the base standard for the pigments recipes, although they vary in their components (see Table 1).

In the first two shelters (Cueva Grande and Cueva en el Medio) it is evident the importance of red color (hematite) while in Cueva Pequeña the choice of material for the painting is the black (charcoal). However, it

Table 1
Combined representation of the results and attempted interpretation.

Shelter	Samples	Description	Micro-Raman	ATR-FTIR	Pigments
Cueva Grande	BSQG-1	Red Figure	Hematite + Oz	Qz (heated; it may be from the rock composition itself).	Hematite
	BSQG-2	Red figure	Hematite	Qz + Hematite	Hematite
	BSQG-3	Brown figures	Hematite	Clay + Oleic acid	Red Ochre + Organics (Oleic acid) (aldehyde = plants)
	BSQG-4		Hematite	Qz + Hematite + Clay + Phosphates	
Cueva en el Medio	BSQM-1	Red Eye-shaped idol figure	Hematite	Qz	Hematite
	BSQM-2	Red fingerprints	Hematite + Qz	Clay + Organics	Ochre + Organics
	BSQM-3	Red fingerprints	Hematite	Qz	Hematite
	BSQM-4	Red figure	Hematite + Clay	Organics	Hematite + Clay + Organics
	BSQM-5	Thick red figure	Hematite	Qz	Hematite
	BSQM-6	Thick circular red figure	Hematite	Red Ochre + Organics	Red Ochre + Organics
Cueva Pequeña	SAMPLE 1	Black fingerprints	Carbon/ Charcoal	Not analyzed	Charcoal
	SAMPLE 2	Black fingerprints	Carbon/ Charcoal	Not analyzed	Charcoal
	SAMPLE 3	Black lines	Carbon/ Charcoal	Not analyzed	Charcoal

is also evident that both techniques and recipes present some variations which could indicate cultural and or symbolic choices.

In Cueva Grande both samples from inside the shelter (BSQG-1 and BSQG-2) seem to be made by using hematite without any mixture. However, the sample from the exterior panel (BSQG-3) clearly was made using different material: the figure presents a different color (brown) and its composition is clearly different because clay has been used as pigment mixed with an organic component probably from vegetal origin.

In Cueva en el Medio, the most important figure of the shelter is the red eye-shape idol figure (BSQM-1). The results for this figure show only hematite for sampling limitation in ATR-FTIR. The fingerprints near this figure (BSQM-2) are made of red color mixed with organics of probable vegetal origin, as it has been found in other pigment of Iberian Peninsula (Oliveira et al., 2017). A trace of clay has also been identified in this sample. Sample 6 (BSQM-6) a thick red figure was found with components such us dehydrated clay (red ochre) and a nitrogen substance (non-volunteer).

The pattern presented seems to be clear: the use of hematite mixed with clay or red ochre both using organic substances probably as binders. While it appears to be evident the presence of a pattern of use of certain ingredients for the manufacture of pigment, the types used are different. In all samples where the standard hematite + organic + clay or red ochre with organic is used, neither the clays nor the organic substances seems to be the same. Despite this, the organic substances appear to be all of plant origin, but of different types.

Taking into account the results, we may question the use of a certain pigment pattern for the first two shelters and a completely different painting pattern and application for the Cueva Pequeña shelter. It is possible to dispute about the use of space made by different groups or in different chronologies by the same group. The use of different types of both clay and organic is very interesting since the main elements are the same.

There are at least three recipes, all mixed clay with organics. It seems that vegetable substances are preferred to animal ones.

These results matches with the majority of analysis realized in Iberia Peninsula where the red pigments are based on hematite and black is normally charcoal (Hernanz et al., 2008). In few cases it was recognized organic matter (Oliveira et al., 2017; López-Montalvo et al., 2017).

Declarations

Author contribution statement

Rosina P., Collado H., Garcês S., Gomes H., Eftekhari N., Nicoli M., Vaccaro C: Conceived and designed the experiments; Performed the experiments; Analyzed and interpreted the data; Contributed reagents, materials, analysis tools or data; Wrote the paper.

Funding statement

Sara Garcês benefits from a Research Fellowship in the Scientific Area of Holocene Archaeology and Rock Art of Tagus Valley in the scope of the Tomar Polytechnic Institute through the FCT - Foundation for Science and Technology - funding at the Geosciences Center of the University of Coimbra (Project UID/Multi/00073/2013). This research was undertaken as part of the strategic programme of the Instituto Terra e Memória and the Geosciences Centre of Coimbra University, Portugal, having benefitted from the financial support of FCT-MEC through national funds and, when applicable, co-financed by FEDER in the ambit of the partnership PT2020, through the research project UID/Multi/00073/2013 of the Geosciences Centre.

Competing interest statement

The authors declare no conflict of interest.

Additional information

No additional information is available for this paper.

Acknowledgements

The authors thank Dr Vitor Gaspar from the Laboratory of Physics and Chemistry and X-Ray (Tomar Polytechnic Institute).

References

Bikiaris, D., Daniilia, S., Sotiropoulou, S., Katsimbiri, O., Pavlidou, E., Moutsatsou, A.P., Chryssoulakis, Y., 2000. Ochre-differentiation through micro-Raman and micro-FTIR spectroscopies: application on wall paintings at Meteora and Mount Athos, Greece. Spectrochim. Acta A 56, 3–18.

Buzgar, N., Buzatu, A., Sanislav, I.V., 2009. The Raman study on certain sulfates. Analele Stiintifice ale Universitatii. Al. I. Cuza 55, 5–23.

Chakraborty, A.K., Ghosh, D.K., 1991. Interpretation on the changes of co-ordination number of al in the thermal changes of kaolinite. Clay Sci. 8, 45–57.

Che, C., Glotch, T.D., Bish, D.L., Michalski, J.R., Xu, W., 2011. Spectroscopic study of the dehydration and/or dehydroxylation of phyllosilicate and zeolite minerals. J. Geophys. Res. 116, E05007.

Ch'ng, Y.S., Tan, C.S., Loh, Y.C., Ahmad, M., Zaini Asmawi, M., Yam, M.F., 2016. Vasorelaxation study and tri-step infrared spectroscopy analysis of Malaysian local herbs. J. Pharmacopuncture 19 (2), 145–154.

Coccato, A., Jehlicka, J., Moens, L., Vandenabeele, P., 2014. Raman spectroscopy for the investigation of carbon-based black pigments. J. Raman Spectrosc. 46, 1003–1015.

Cornell, R.M., Schwertmann, U., 2006. The Iron Oxides: Structure, Properties, Reactions, Occurrences and Uses. Wiley-VCH, Weinheim.
Eastaugh, N., Walsh, V., Chaplin, T., Siddall, R., 2008. Pigment Compendium. A Dictionary and Optical Microscopy of Historical Pigments. Elsevier Butterworth-Heinemann, Oxford, UK.
Ekosse, G.-L., 2005. X-Ray Powder Diffraction Patterns of Clays and Clay Minerals in Botswana. X-Ray Diffraction Unit, University of Botswana, Ilustrada, 78p.
Franquelo, M.L., Duran, A., Herrera, L.K., Jimenez de Haro, M.C., Perez-Rodriguez, J.L., 2009. Comparison between micro-Raman and micro-FTIR spectroscopy techniques for the characterization of pigments from Southern Spain Cultural Heritage. J. Mol. Struct. 924–926, 404–412.
Froment, F., Tournié, A., Colomban, P., 2008. Raman identification of natural red to yellow pigments: ochre and iron-containing ores. J. Raman Spectrosc. 39, 560–568.
Frost, R.L., Kristof, J., Horvath, E., Martens, W., Kloprogge, T., 2002. Complexity of intercalation of hydrazine into kaolinite - a controlled rate thermal analysis and DRIFT spectroscopic study. J. Colloid Interface Sci. 251 (2), 350–359.
Gomes, H., Rosina, P., Holakooei, P., Solomon, T., Vaccaro, C., 2013. Identification of pigments used in rock-art paintings in Gode Roriso-Ethiopia using Micro-Raman spectroscopy. J. Archaeol. Sci. 40, 4073–4082.
Hanesch, M., 2009. Raman spectroscopy of iron oxides and (oxy)hydroxides at low laser power and possible applications in environmental magnetic studies. Geophys. J. Int. 177, 941–948.
Hernanz, A., Gavira-Vallejo, J.M., Ruiz-López, J.F., Edwards, H.G.M., 2008. A comprehensive micro-Raman spectroscopic study of prehistoric rock paintings from the Sierra de las Cuerdas, Cuenca, Spain. J. Raman Spectrosc. 39, 972–984.
Hernanz, A., Gavira-Vallejo, J.M., Ruiz-López, J.F., Martin, S., Maroto-Valiente, Á., De Balbín-Behrmann, R., Menédez, M., Alcolea-González, J.J., 2012. Spectroscopy of palaeolithic rock paintings from the Tito Bustillo and el Buxu caves, Asturias, Spain. J. Raman Spectrosc. 43, 1644–1650.
Hu, Y., Fitzgerald, N., Guocheng, L., Xing, X., Wei-Teh, J., Zhaohui, L., 2015. Adsorption of atenolol on kaolinite. Advances in Materials Science and Engineering 2015. Article ID 897870, 8 pages.
Hunt, A., Thomas, P., James, D., David, B., Geneste, J., Delannoy, J., Stuart, B., 2018. The characterisation of pigments used in X-ray rock art at Dalakngalarr 1, central-western Arnhem Land. Microchem. J. 126 (2016), 524–529.
Iriarte, E., Foyo, A., Sánchez, M.A., Tomillo, C., 2009. The origin and geochemical characterization of red ochres from the Tito Bustillo and Monte Castillo caves (Northern Spain). Archaeometry 51 (2), 231–251.
Iriarte, M., Hernanz, A., Ruiz-López, J.F., Martin, S., 2013. μ-Raman spectroscopy of prehistoric paintings from the Abrigo Remacha rock shelter (Villaseca, Segovia, Spain). J. Raman Spectrosc. 44, 1557–1562.
Iriarte, M., Hernanz, A., Gavira-Vallejoa, J.M., Alcolea-González, J., de Balbín-Behrmannb, R., 2017. μ-Raman spectroscopy of prehistoric paintings from the El Reno cave (Valdesotos, Guadalajara, Spain). J. Archaeol. Sci. Report 14, 454–460.
Legodi, M.A., Waal, D., 2006. The preparation of magnetite, goethite, hematite and maghemite of pigment quality from mill scale iron waste. Dyes Pigments 74, 161–168.
López-Montalvo, E., Roldán, C., Badal, E., Murcia-Mascarós, S., Villaverde, V., 2017. Identification of plant cells in black pigments of prehistoric Spanish Levantine rock art by means of a multi-analytical approach. A new method for social identity materialization using *chaîne opératoire*. Petraglia MD, ed. PLoS One 12 (2), e0172225.
Niederb, J., Todt, B., Boca, A., Nitschke, R., Kohler, M., Kühn, P., Bauhus, J., 2015. Use of near-infrared spectroscopy to assess phosphorus fractions of different plant availability in forest soils. Biogeosciences 12, 3415–3428.
Oliveira, C., Bettencourt, A.M.S., Araújo, A., Gonçalves, L., Kuzniarska-Biernacka, I., Costa, L., 2017. Integrated analytical techniques for the study of colouring materials from two megalithic barrows. Archaeometry.
Omotoso, M., Ajagum, S., 2016. Graft copolymerization of methlymethacrylate on lignin produced from agricultural wastes. Int. J. Chem. 8 (2).
Pavón Soldevila, I., Duque Espino, D.M., Sanabria Murillo, D., y Collado Giraldo, H., 2018. "La estela de 'Cabeza del Buey V/El Palacio' en el poblamiento de la Edad del Bronce de la sierra de Tiros (Badajoz)". Spal 27 (1), 31–60.
Pietro, A.C., Jimenez, J., 2000. Analytical techniques for characterizing polychromated coatings on quartzite samples from a prehistoric cave. In: Fassina, V. (Ed.), Proceedings of the 9th International Congress on Deterioration and Conservation of Stone, first ed. Elsevier Science, pp. 619–628.
Prinsloo, L., Toumié, A., Colombam, P., Paris, C., Bassett, S., 2013. In search of the optimum Raman/IR signatures of potential ingredients used in San/Bushman rock art paint. J. Archaeol. Sci. 40 (7), 2981–2990.
Rospenk, M., Zeegers-Huyskens, T., 1997. FT-IR (7500−1800 cm-1) study of hydrogen-bond complexes between Phenols−OH(OD) and pyridine. Evidence of proton transfer in the second vibrational excited state. J. Phys. Chem. A 101 (45), 8428–8434.
Rousaki, A., Bellelli, C., Carballido Calatayud, M., Aldazabal, V., Custo, G., Moens, L., Vandenabeelee, P., Vázquez, C., 2015. Micro-Raman analysis of pigments from hunter–gatherer archaeological sites of North Patagonia (Argentina). J. Raman Spectrosc. 46, 1016–1024.
Sathya, P., Velraj, G., Meyvel, S., 2012. Fourier transform infrared spectroscopic study of ancient brick samples from Salavankuppam Region, Tamilnadu, India. Adv. Appl. Sci. Res. 3 (2), 776–779.
Schiegl, S., Conard, N.J., 2006. The Middle Stone Age sediments at Sibudu: results from FTIR spectroscopy and microscopic analyses. South. Afr. Humanit. 18 (1), 149–172. Pietermaritzburg.
Schuttlefield, J., Cox, D., Grassian, V., 2007. An investigation of water uptake on clays minerals using ATR-FTIR spectroscopy coupled with quartz crystal microbalance measurements. J. Geophys. Res. 112 (D21303), 1–14.
Wainright, I.N.M., Helwig, K., Rolandi, D.S., Gradin, C., Podestá, M.M., Onetto, M., Achero, C.A., 2002. Rock paintings conservation and pigment analysis at Cueva de las Manos and Cerro de los Indios, Santa Cruz (Patagonia). In: Vontobel, R. (Ed.), ICOM Committee for Conservation, 13th Triennial Meeting, Rio de Janeiro, 22–27 September 2002, James and James. Science Publishers, London, pp. 582–589.
Zuo, J., Xu, C., Wang, C., Yushi, Z., 1999. Identification of the pigment in painted pottery from the xishan site by Raman microscopy. J. Raman Spectrosc. 30, 1053–1055.